

## A Theoretical Study of the Reaction between $N^+(^3P)$ and Formaldehyde and Related Processes in the Gas Phase

Fatima Ijjaali,<sup>†</sup> Manuel Alcamí, Otilia M6, and Manuel Yáñez\*

Departamento de Química, C-9, Universidad Autónoma de Madrid, Cantoblanco, 28049-Madrid, Spain

Received: June 27, 2000; In Final Form: September 20, 2000

The  $[H_2, C, N, O]^+$  potential energy surface (PES) in its triplet state multiplicity has been explored by means of high-level ab initio calculations, carried out in the framework of the G2 theory. From the PES survey we conclude that some of the products of the  $N^+(^3P) + H_2CO$  reaction are the result of a competitive dissociation of the  $H_2CON^+$  cation into  $NO^+ + H_2C$  or  $N + H_2CO^+$ . Although the first process is more exothermic than the second one, it involves a conical intersection, and as a consequence  $N + H_2CO^+$  are the dominant products.  $NH + HCO^+$ , which are also experimentally observed products, can be formed either by the dissociation of the  $HCONH^+$  cation, through another conical intersection, or by the fragmentation of a quite stable  $HN\cdots HCO^+$  complex. Other possible products, such as  $CNH + OH^+$ ,  $HCN + OH^+$ , and  $CO + NH_2^+$ , although exothermic, should not be observed since the corresponding reaction pathways involve high activation barriers. These conclusions are in good agreement with the experimental evidence. The topology of the  $[H_2, C, N, O]^+$  PES also explains why no reaction is observed when  $NH_2^+$  and  $CO$  or  $CH_2$  and  $NO^+$  interact in the gas phase, while in  $CH_2^+ + NO$  reactions, only the charge exchange channel is open. We also predict that the dominant products in  $OH^+ + HCN$  reactions should be  $NH + HCO^+$ . However, when this reaction involves the  $CNH$  isomer the observed products should be not only  $NH + HCO^+$  but also  $NH_2^+ + CO$ .

### Introduction

In the past decades a good deal of attention was directed toward gaining an understanding of the reactions between ions, mainly monocations, and neutral molecules.<sup>1</sup> This interest was motivated, among other reasons, by the importance of these reactions to understand the chemistry of the Earth's atmosphere or to envisage the mechanisms responsible for the formation of many interstellar chemical species.<sup>2</sup> It is important to emphasize that insight into the mechanisms by which ion–molecule reactions proceed at thermal energies has been very often the result of an adequate combination of experimental and theoretical information. The availability of very accurate ab initio methods<sup>3</sup> has been of great relevance, since nowadays it is not only possible to explore the whole potential energy surface (PES) associated with a given reaction, and therefore to have a good knowledge of its mechanism, but also to estimate, with reasonably high accuracy, the heats of formation of atmospheric or interstellar species which are not amenable for experiment.

In our group we have paid some attention<sup>4</sup> to these kinds of reactions in particular when the reactant monocation is an open-shell species.

The aim of the present paper is to investigate, through the use of high-level ab initio techniques the PES associated with the reactions between  $N^+$  in its triplet ground state and formaldehyde. This reaction is of particular interest in atmospheric chemistry, in particular in the *D* region of the stratosphere,<sup>5</sup> whose ion chemistry is expected to be dominated by minor neutral constituents, which either diffuse from the Earth's surface or are synthesized in the stratosphere. This is the case of formaldehyde, which can be produced in this region by oxidation of  $CH_4$  previously formed in the Earth's surface.

On the other hand, ionization processes mainly produced by cosmic rays are also frequent in the stratosphere, the main product ions being  $N^+$ ,  $N_2^+$ ,  $O^+$ , and  $O_2^+$  since nitrogen and oxygen are the main constituents of our atmosphere. However, the terminating ion species are the result of the reactions of the aforementioned ions mainly with water vapor, but also with minor constituents, one of which is formaldehyde.

The reaction between  $N^+$  and  $H_2CO$  has been experimentally studied by means of selected ion flow tube (SIFT) techniques.<sup>6</sup> However, to the best of our knowledge the mechanism of this process has never been investigated before. Furthermore, estimating the relative proportions of  $H_2CO^+$  and  $NO^+$  (both 30 amu) from the mass spectrometry techniques used<sup>7</sup> was not an easy task. In fact, although this experimental study concluded that the main products are  $H_2CO^+$  (65%),  $HCO^+$  (25%), and  $NO^+$  (10%), the proportion in which  $H_2CO^+$  and  $NO^+$  are formed are only accurate<sup>6</sup> within a factor of 2.

It is worth also noting that the PES associated with the aforementioned reaction is common to other important processes in astrochemistry. Hence, the following reactions  $NO + CH_2^+$ ,  $CO + NH_2^+$ ,  $HCN + OH^+$ , and  $CNH + OH^+$  will be also discussed along this paper.

### Computational Details

Standard G2 ab initio calculations have been performed using the Gaussian 98 series of programs.<sup>7</sup> The G2 approach is a composite procedure which yields final energies of an effectively QCISD(T)/6-311+G(3df,2p) quality, assuming that basis set effects on the correlation energies are additive. A small empirical correction (HLC) to accommodate remaining deficiencies is finally added as well as the corresponding zero point energy (ZPE) correction, estimated at the HF/6-31G\* level. The reader is addressed to ref 3a for a complete description of this method,

<sup>†</sup> Permanent address: Département de Chimie, Faculté des Sciences-Semlalia, BP: 2390 40002 Marrakesh, Morocco.

**TABLE 1: G2 Total Energies of the Different  $[\text{H}_2, \text{C}, \text{N}, \text{O}]^+$  Triplet-State Cations,  $E(\text{G2})$  (hartrees)**

system	$E(\text{G2})$	system	$E(\text{G2})$
1	-168.521 236	TS1-2	-168.445 737
2	-168.484 372	TS2-3	-168.445 351
3	-168.490 881	TS3-4	-168.460 977
4	-168.507 313	TS3-5	-168.453 675
5	-168.564 573	TS4-6	-168.443 056
6	-168.555 467	TS4-7	-168.430 943
7	-168.450 016	TS4-8	-168.402 170
8	-168.499 595	TS6-8	-168.438 742
9	-168.465 990	TS7-8	-168.390 412
10	-168.448 340	TS1-9	-168.438 053
11	-168.568 613	TS9-3	-168.433232
12	-168.569 777	TS9-6	-168.421 798
13	-168.560 583	TS9-10	-168.40 7553
14	-168.584 662	TS10-11	-168.434 721
15	-168.446 055	TS11-12	-168.537 281
CI1	-168.464 666	TS12-13	-168.490 586
CI2	-168.438 357	TS12-5	-168.524 036
		TS5-13	-168.501 941
		TS13-14	-168.500 816
		TS3-15	-168.361 196
		TS15-14	-168.394 867

which provides thermodynamic properties as heats of formation, protonation energies, ionization potentials, etc., within chemical accuracy.

As we shall discuss in forthcoming sections, some reactive channels involved conical intersections between different triplet states. To locate these conical intersections we have used the procedure developed by Bearpark et al.,<sup>8</sup> as implemented in the Gaussian 98 series of programs.<sup>7</sup> For this purpose we have used initially a CASSCF procedure with an active space which includes six electrons and five orbitals. The basis set expansion used was 6-31G\*. The initial geometry so obtained was then refined at the QCISD/6-311+G(d,p) level of theory to obtain the structure of the corresponding transition state. For the sake of consistency the final energy was evaluated at the G2 level, but keeping frozen the QCISD optimized geometry.

The bonding characteristics of the different local minima were analyzed by means of two different partition techniques, namely, the natural bond orbital (NBO) analysis of Weinhold et al.,<sup>9</sup> which usually provides reliable atomic charges, and the atoms in molecules (AIM) theory of Bader,<sup>10</sup> which offers a good procedure to analyze the nature of the bonds within a chemical system. The AIM formalism is based in a topological analysis of the electron charge density  $\rho(\mathbf{r})$  and its Laplacian  $\nabla^2\rho(\mathbf{r})$ . It is well established that the values of  $\rho$ ,  $\nabla^2\rho$ , and the energy density<sup>11</sup>  $H(\mathbf{r})$  at the bond critical points provide useful information on bonding characteristics. In most cases negative values of the Laplacian are associated with covalent linkages, while positive values are usually associated with closed-shell interactions as those found in ionic bonds, van der Waals complexes, and hydrogen bonds. Although the Laplacian can exhibit significant exceptions to this general rule, the energy density does not, so negative values of  $H(\mathbf{r})$  are always associated with covalent linkages<sup>11</sup> even in those particular cases, as the  $\text{F}_2$  molecule, where the Laplacian is positive. Since as mentioned above, electron correlation effects are crucial for the systems under investigation, these population analyses were carried out at the MP2 level. The AIM analysis was performed by using the AIMPACK set of programs.<sup>12</sup>

## Results and Discussion

The total energies of the different  $[\text{H}_2, \text{C}, \text{N}, \text{O}]^+$  triplet state cations are summarized in Table 1. The structures of the minima

**TABLE 2: Bonding Characteristics of  $[\text{H}_2, \text{C}, \text{O}, \text{N}]^+$  Triplet State Cations in Terms of the Charge Density  $\rho(\mathbf{r})$  and the Energy Density  $H(\mathbf{r})$  Evaluated at the Corresponding Bond Critical Points (all values in au)**

	CO		NO		NC	
	$\rho(\mathbf{r})$	$H(\mathbf{r})$	$\rho(\mathbf{r})$	$H(\mathbf{r})$	$\rho(\mathbf{r})$	$H(\mathbf{r})$
0	0.430	-0.714				
1	0.344	-0.553	0.287	-0.270		
2	0.374	-0.606	0.236	-0.187		
3	0.233	-0.317	0.341	-0.357	0.281	-0.447
4			0.396	-0.440	0.379	-0.669
5	0.473	-0.808			0.024	0.002
6			0.539	-0.810	0.320	-0.537
7			0.377	-0.419	0.282	-0.449
8			0.413	-0.486	0.361	-0.628
9	0.257	-0.382	0.212	-0.140	0.321	-0.455
10	0.222	-0.297	0.227	-0.169	0.283	-0.335
11	0.351	-0.576			0.347	-0.449
12	0.350	-0.575			0.343	-0.446
13	0.354	-0.574			0.341	-0.546
14	0.442	-0.747			0.200	-0.171
15	0.284	-0.447	0.245	-0.187	0.265	-0.410

of the PES are given in Figure 1, while Figure 2a,b contains the energy profile associated with the  $N^+(\text{}^3\text{P}) + \text{H}_2\text{CO}$  reaction.

**Structures and Bonding.** Although a detailed description of the structures of the different  $[\text{H}_2, \text{C}, \text{N}, \text{O}]^+$  triplet state cations is not the main goal of this work there are some points that deserve to be singled out for comment. In the first place, the interaction between  $N^+(\text{}^3\text{P})$  and formaldehyde yields covalently bound species. This is at variance with what was found for other triplet state cations as  $\text{F}^+$  and  $\text{Cl}^+$ , where the interactions yield systematically weakly bound species.<sup>4c,e-g</sup> The interaction between  $N^+$  and neutral formaldehyde can be envisaged as a two-steps process. The first one corresponds to a charge transfer, due to the high recombination energy of  $N^+(\text{}^3\text{P})$ . As a result, a neutral nitrogen atom, in its quartet ground state, will be formed, while the  $\text{H}_2\text{CO}^+$  moiety would be a doublet state cation. To preserve the overall triplet multiplicity of the entrance channel, the spin of the unpaired electrons in N must be opposite to that of  $\text{H}_2\text{CO}^+$  moiety, favoring the formation of a covalent linkage between both subunits in the second step. This possibility is forbidden in halogen cation reactions<sup>4c,e-g</sup> because, although the charge transfer process is also the primary mechanism, the neutral halogen atom is formed in its doublet ground state and therefore has only one unpaired electron which, to preserve the overall triplet multiplicity, cannot be paired with that of the radical cation. As a consequence the interaction between both subunits is essentially electrostatic.

In the second place it is also worth noting that, the  $N^+(\text{}^3\text{P})$  attachment involves a drastic electron redistribution of the neutral. As illustrated in Table 2, on going from formaldehyde (**0**) to species **1**, there is a significant weakening of the C–O bond, since part of the electron density in the C–O bonding region is used to form the new covalent N–O linkage. Consistently, the C–O stretching frequency is red-shifted by  $534\text{ cm}^{-1}$ , while the bond length increases  $0.04\text{ \AA}$ .

This CO bond weakening is quite important from the reactivity point of view since will favor the C–O bond fission, yielding  $\text{NO}^+ + \text{CH}_2$  which are some of the experimentally observed products in  $N^+(\text{}^3\text{P}) + \text{H}_2\text{CO}$  reactions. It should also be noted that according to the AIM analysis the N–O bond is significantly weaker than those found for the other cations of the same potential energy surface, as structures **4** or **6** (see Figure 1 and Table 2). Accordingly, the N–O stretch of species **1** appears at a much lower frequency ( $805\text{ cm}^{-1}$ ) than the same

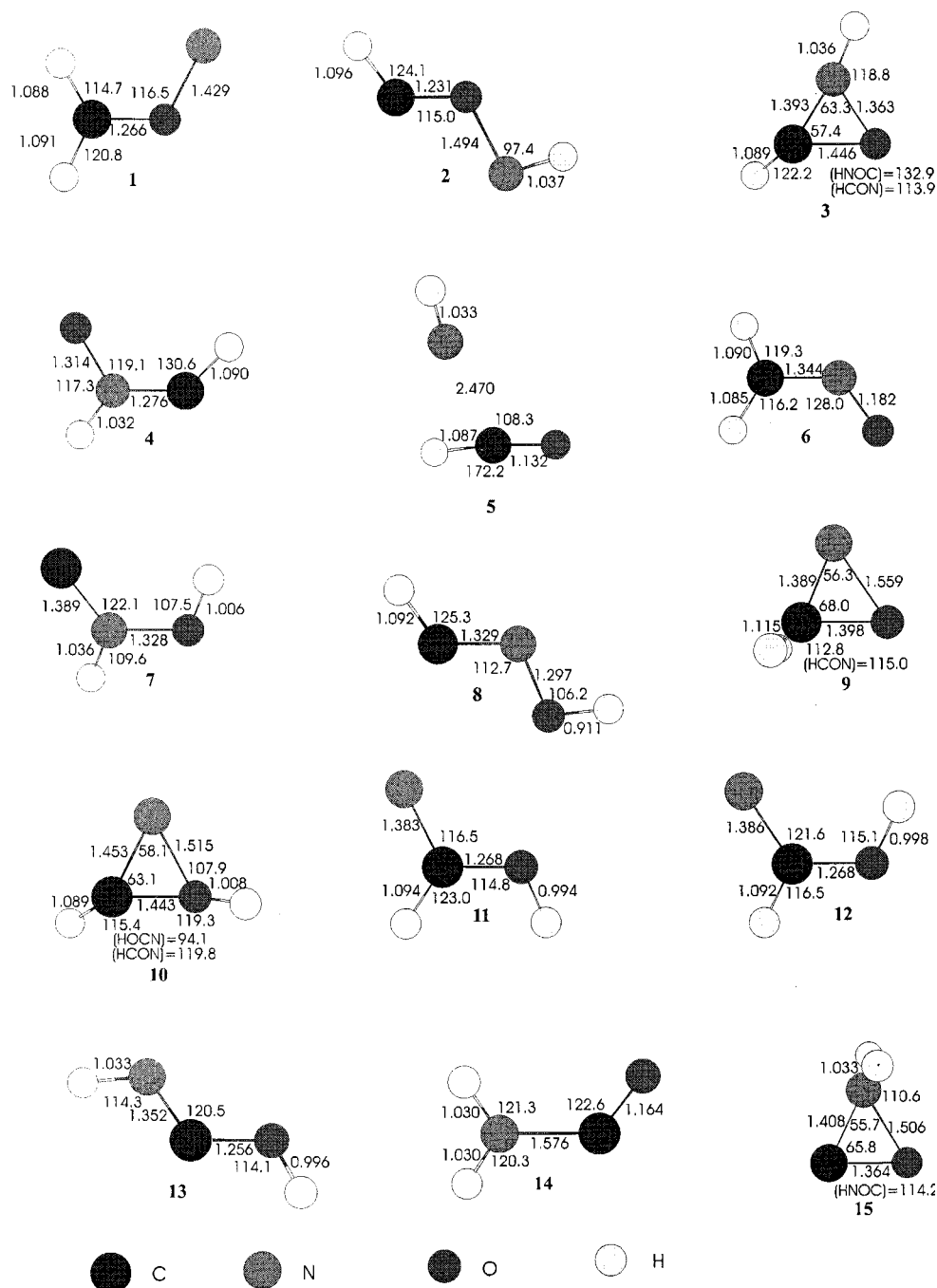


**Figure 1.** MP2/6-31G\* optimized geometries of the different local minima of the  $[H_2C,N,O]^+$  triplet potential energy surface. Bond lengths are in angstroms, and bond angles are in degrees.

vibration in species **4** ( $1048\text{ cm}^{-1}$ ) or in species **6** ( $1493\text{ m}^{-1}$ ). This indicates that species **1** can be also a good precursor for the loss of N yielding  $H_2CO^+$ , which is also one of the experimentally observed products. We will discuss later on these two possibilities in more detail.

As reflected by the charge densities at the corresponding bond critical points, the **1**–**2** isomerization process implies a reinforcement of the C–O bond, while the O–N linkage becomes still weaker (see Table 2). Consistently, the C–O stretching frequency is blue-shifted by  $217\text{ cm}^{-1}$ , while the N–O stretching frequency is red-shifted by  $162\text{ cm}^{-1}$ . As we shall discuss later, as a consequence of this weakening of the N–O linkage, structure **2** becomes a suitable precursor for the NH loss, also observed experimentally. Another precursor for the loss of NH is the local minimum **5**. From the values in Table 2, it can be

seen that the charge density at the C–N bond critical point is rather small and that the energy density is positive, indicating that this structure is an ion–dipole complex between NH and  $HCO^+$ . Consistently, the C–N stretching frequency is predicted to be significantly small ( $168\text{ cm}^{-1}$ ).

Finally, it can be also observed that the global minimum **14** presents a rather weak C–N linkage (see Table 2), while the C–O bond is stronger than that of neutral formaldehyde and almost as strong as that of  $HCO^+$ . In fact, structure **14** could be envisaged as a complex between carbon monoxide and  $NH_2^+$ , the interaction energy being  $18.1\text{ kcal/mol}$ . The negative value of the energy density indicates that this interaction has a non negligible covalent character. In light of these arguments, the global minimum should be an adequate precursor for the loss

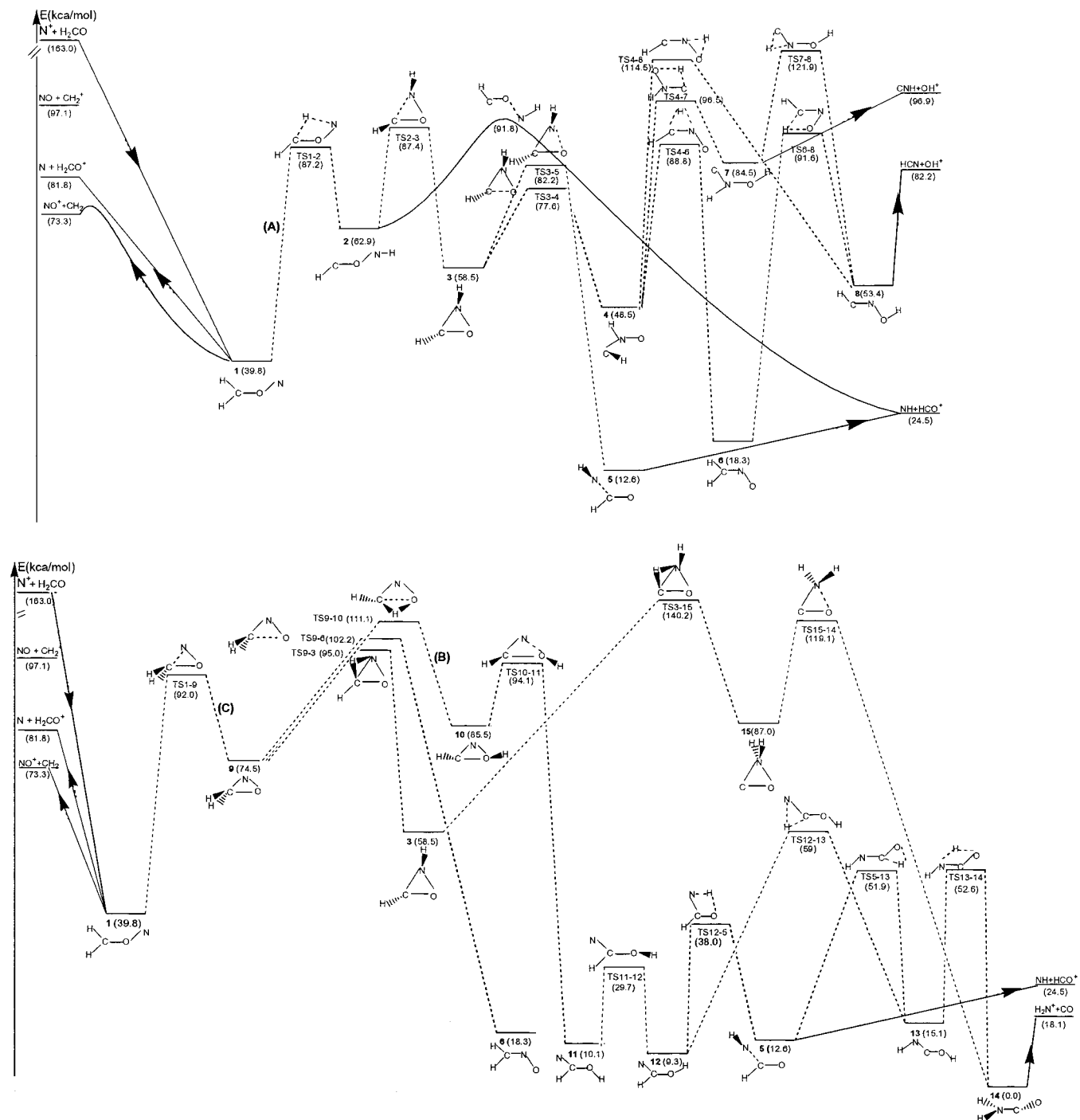


**Figure 2.** Energy profiles associated with: (a) mechanism A, whose first step corresponds to a 1,3-H shift from structure **1**; (b) mechanism B, whose first step is the cyclization of structure **1**.

of CO. However, as we shall discuss in forthcoming sections, this reactive channel will not be accessible in  $N^+(\text{}^3\text{P}) + \text{H}_2\text{CO}$  reactions.

**[H<sub>2</sub>, C, N, O]<sup>+</sup> Potential Energy Surface.** To describe the [H<sub>2</sub>, C, N, O]<sup>+</sup> potential energy surface we shall begin by structure **1** which results from the attachment of the N<sup>+</sup> cation to the oxygen atom of the neutral. We have mentioned above that this structure, although it is not the global minimum of the PES, plays a key role in the reactivity of formaldehyde with respect to N<sup>+</sup>.

Once structure **1** is formed three different mechanisms, namely a 1,3-H shift, a 1,2-H shift and the cyclization of the system to yield a three-membered ring, are, in principle, possible.

**1,3-H Shift from 1.** The 1,3-H shift (mechanism A in Figure 2a) connects the local minimum **1** with structure **2**. As discussed above this process involves a significant reinforcement of the C–O bond, while the O–N linkage becomes weaker. A shortening of the C···N distance, through the TS2–3 transition state, leads to the three-membered cycle **3**, which implies a stabilization of the system by 4.4 kcal/mol. The existence of cyclic structures, such as species **3**, is rather important since they usually favor an easy scrambling of the heavy atoms of the system. Indeed, structure **3** can undergo three different bond fissions. The less favorable one would be precisely the breaking of the C–N bond going backward to structure **2**. The N–O bond fission would yield the local minimum **5**. The C–O bond cleavage is the most favorable of the three to yield structure **4**.

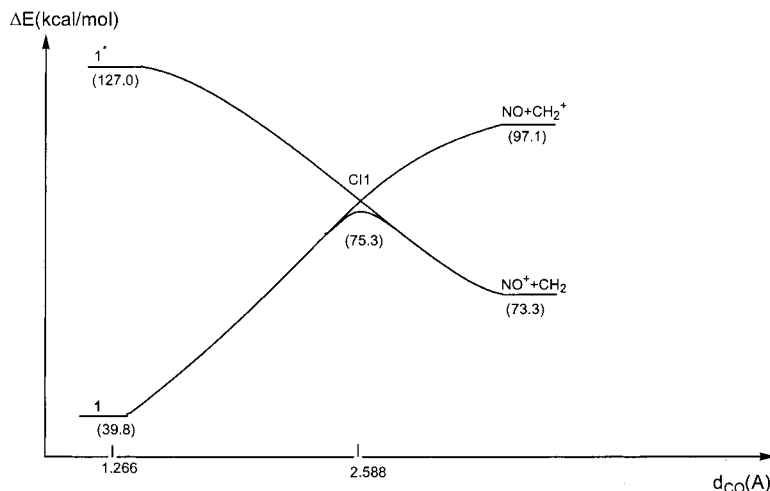


**Figure 3.** Conical intersection (CI) corresponding to the dissociation of species **1** into  $\text{CH}_2 + \text{NO}^+$ . The energy of the corresponding transition state was obtained at the G2 level using QCISD/6-311+G(d,p) optimized geometries. Values relative to the global minimum of the PES.

Structure **4** can undergo three isomerization processes: (a) A 1,3-H shift would yield species **7** which would eventually dissociate into  $\text{CNH} + \text{OH}^+(\Sigma)$ . Actually, our results indicate that species **7** can be viewed as a tightly bound complex between these two subunits, the interaction energy being 12.4 kcal/mol. (b) A H shifting from the NH group toward the CH to yield the local minimum **6** which is the most favorable one. A subsequent 1,3-H shift would connect structures **6** and **8**. (c) The **4–8** isomerization process through the transition state **TS4-8**. Species **8** can be envisaged as a tightly bound complex between HCN and  $\text{OH}^+$ , the interaction energy being 28.8 kcal/mol.

**1,2-H shift from 1.** The 1,2-H shift should yield a  $[\text{HC}-\text{OH}-\text{N}]^+$  cation. However this is not a local minimum of the PES as it collapses to the cyclic structure **10**. This means that the 1,2-H shift must be preceded by a cyclization of the system, yielding structure **9** (see Figure 2b).

Structure **9** may undergo three different bond fissions or two 1,2-H shifts (see Figure 2b). The 1,2-H shift, through the **TS9-10** transition state, leads to structure **10** and implies one of the highest activation barrier of the whole potential energy surface. Therefore, the structures along this path (mechanism B) should not play any relevant role in  $\text{N}^+ + \text{CH}_2\text{O}$  reactions, even though the N–O bond cleavage would connect structure **10** with a very stable cation **11**. This cation has two nonequivalent conformers depending on the relative position of the hydrogen atom of the OH group, the most stable one being that in which this hydrogen atom is *cis* with respect to the nitrogen atom (See Figure 2b). Both isomers are connected through the **TS11-12** transition state which implies the internal rotation of the OH group. A 1,3-H shift leads from **12** to **5** which can be considered as a tightly bound complex between  $\text{HCO}^+$  and NH. It is important to note that structure **5** can also be obtained by the N–O bond fission of the cyclic structure **3** belonging to what we have called mechanism A (see Figure 2a).

Structure **12** is connected with species **13** by a 1,2-H shift, which involves a larger activation barrier. Structure **13** can also be viewed as the result of the isomerization of the  $\text{HCO}^+$  moiety of complex **5** through the **TS5-13** transition state. This isomerization leads to the  $\text{COH}^+$  isomer, which is 37.2 kcal/mol less stable,<sup>13</sup> and to a significant reinforcement of the C–N bond, which now become a covalent linkage. This bond reinforcement explains why, despite the low stability of the  $\text{COH}^+$  moiety, species **13** lies only 2.5 kcal/mol higher in energy than complex **5**. A subsequent 1,3-H shift leads to the global

minimum of the PES **14**, which, as we have mentioned above, would eventually dissociate into  $\text{CO} + \text{NH}_2^+$ .

The second possible 1,2-H shift from structure **9** yields structure **3**, also involved in mechanism A (see Figure 2a). The reaction paths associated with the bond fissions of this cyclic species **3** were discussed above. In Figure 2b, we show that the barrier associated with a possible 1,2-H shift to yield species **15** is very high. Species **15** is connected through the **TS15-14** transition state with the global minimum of the PES.

Let us discuss now the three different bond fissions which can undergo species **9**. The cleavage of the C–O bond, through **TS9-6**, yields structure **6**, which was also found along the mechanism A. The breaking of the C–N permits to go backward to structure **1**. We have not found however any stable structure corresponding to the N–O bond fission, since all attempts collapsed to the cyclic structure **9**.

**$\text{N}^+(\text{^3P}) + \text{H}_2\text{CO}$  Reaction.** Obviously, the first step in  $\text{N}^+ + \text{H}_2\text{CO}$  reactions should correspond to the attachment of the  $\text{N}^+$  to the basic center of the neutral to yield species **1**. Once the molecular cation **1** is formed, it can undergo the isomerizations described in the preceding section or dissociate either into  $\text{H}_2\text{CO}^+ + \text{N}$  or into  $\text{H}_2\text{C} + \text{NO}^+$ . The first important point is that, according to the values of the activation barriers shown in Figures 2a,b, only mechanism A, associated with the 1,3-H shift, can compete with the dissociation into  $\text{H}_2\text{CO}^+ + \text{N}$  or into  $\text{H}_2\text{C} + \text{NO}^+$ . This implies that structure **1** must be the precursor of the main products of the reaction under investigation. The second important point is that dissociation of **1** into  $\text{H}_2\text{C} + \text{NO}^+$  requires less energy than its dissociation into  $\text{H}_2\text{CO}^+ + \text{N}$ . Hence, a naive interpretation of Figure 2a would lead to the conclusion that  $\text{CH}_2 + \text{NO}^+$  should be the dominant products of the reaction. However, the experimental evidence indicates that  $\text{N} + \text{H}_2\text{CO}^+$  are formed in a greater proportion. This clearly indicates that the dissociation of structure **1** into  $\text{CH}_2 + \text{NO}^+$  must involve an activation barrier. In other words, the evolution from **1** to the dissociation products implies the existence of a conical intersection between two triplet states. We have estimated, by means of CASSCF(4,4)/6-311+G(d,p) calculations, that the energy gap between the ground and the first excited state of species **1** is ca. 87 kcal/mol (see Figure 3). This means that the first excited state of this structure is well above both dissociation limits. On the other hand, when the C–N distance increases, the ground state of **1** tends to the  $\text{NO} + \text{CH}_2^+$  dissociation limit while the first excited state tends to  $\text{NO}^+ + \text{CH}_2$ . The corresponding conical intersection (CI)

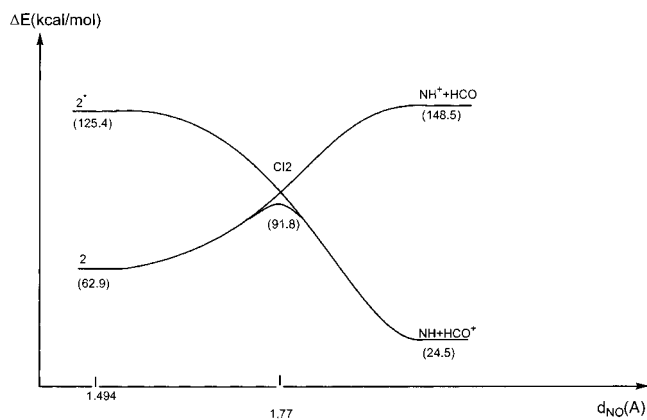


**Figure 4.** Conical intersection (CI2) corresponding to the dissociation of species **2** into  $NH + HCO^+$ . The energy of the corresponding transition state was obtained at the G2 level using QCISD/6-311+G(d,p) optimized geometries. Values relative to the global minimum of the PES.

between both surfaces (See Figure 3) is estimated to take place at a C–N distance of 2.59 Å. Consistently, an inspection of the wave function of the lowest energy state shows that for C–N distances smaller than this value one of the unpaired electrons is located at the nitrogen atom and the other at the carbon atom, while the positive charge is mainly associated with the  $CH_2$  moiety. In contrast, for C–N distances larger than the distance of the conical intersection, both unpaired electrons appear associated with the  $CH_2$  moiety, while the NO subunit is the one which sustains the positive charge. Once this conical intersection was located, we have found that the corresponding transition state lies 2.0 kcal/mol above the  $CH_2 + NO^+$  dissociation limit (see Figure 3).

We have also checked that the dissociation of structure **1** into  $H_2CO^+ + N$  takes place without activation barrier. Hence we must conclude that, although the dissociation into  $NO^+ + CH_2$  is less costly from the energetic point of view than the charge exchange process, the latter could be the most favorable one. This is in agreement with the experimental evidence<sup>6</sup> which estimates that 65% of the reactions products correspond to the charge exchange process and only 10% to  $NO^+ + CH_2$ . This seems a large difference in the light of our results. However, it must be taken into account that, as mentioned in the Introduction, the experimental values are uncertain by a factor of 2.<sup>6</sup>

The PES shown in Figure 2a indicates also that the **1**–**2** isomerization process must compete with the aforementioned dissociations, since the corresponding activation barrier is only 5.4 kcal/mol higher than the  $N + H_2CO^+$  dissociation limit. As we have mentioned above, species **2** is a good precursor for the loss of NH due to the weakness of the C–N linkage. Since the  $HCO^+ + NH$  dissociation limit lies much lower in energy (See Figure 2a), the dissociation of **2** must proceed through an activation barrier. We have found, using the same procedure outlined above for the case of structure **1**, that the first excited state of species **2** lies 62.5 kcal/mol above it. On the other hand, when the C–N bond is enlarged the ground state of species **2** tends toward  $NH^+ + HCO$ , while its first excited state tends to  $NH + HCO^+$ . The conical intersection between both potential energy surfaces (CI2) is estimated to occur for a C–N distance of 1.77 Å. The corresponding transition state for this dissociation process was estimated to be 28.9 kcal/mol above structure **2** (see Figure 4).

Alternatively, species **2** can evolve to yield structure **3**. This process involves an activation barrier of 24.5 kcal/mol and therefore should be slightly favored with respect to the dis-

sociation into  $HCO^+ + NH$ . The important point, however, is that this alternative pathway leads the same final products. In fact, as shown in Figure 2a, once species **3** is formed the most favorable evolution should yield **5**, which would eventually dissociate into  $NH + HCO^+$ , since the pathway via structure **4** involves much higher activation barriers.

In summary, we must conclude that the formation of  $NH + HCO^+$  as reaction products can be the result of a direct dissociation of species **2**, involving a conical intersection, or the consequence of its isomerization to yield structure **3**, and subsequently structure **5**, which eventually dissociates.

Finally, it must be observed that all the alternative structures **4**, **6**, **8**, **13**, or **14** should not be accessible since the corresponding pathways involve higher activation barriers than those discussed above. Therefore, we must conclude that  $HNC + OH^+$ ,  $CNH + OH^+$ , or  $CO + NH_2^+$  should not be observed as products in  $N^+ + H_2CO$  reactions, in agreement with the experimental evidence. Nevertheless, those structures will play significant roles in other reaction processes which will be analyzed in forthcoming sections.

**$NH_2^+(^3B_1) + CO$  Reactions.** As shown in Figure 2b, the interaction between  $NH_2^+$  and carbon monoxide leads to the formation of a tightly bound complex **14**, which lies 18.1 kcal/mol lower in energy. However, the most conspicuous fact is that the isomerization processes which can undergo this complex require activation barriers which are much higher in energy than the entrance channel. Hence, the most likely process would be its dissociation into the reactants. This is in agreement with the experimental observation<sup>14</sup> which indicates that there is no reaction between  $NH_2^+$  and CO in the gas phase.

**$OH^+(^3\Sigma) + CNH$  and  $OH^+(^3\Sigma) + HCN$  Reactions.** For the sake of clarity we have redrawn in Figure 5 part of the PES of Figure 2 which is relevant to understand the possible mechanisms associated with these two reactions.

In principle, the first step in any of these two processes would be the attachment of the  $OH^+$  cation to one of the basic centers of the neutral. Our results clearly show that in both cases the attachment to the carbon atom is much more favorable than the attachment to the nitrogen atom. Hence, in the reaction between  $OH^+ + HCN$ , the formation of species **12** is strongly favored, and only very small amounts, if any, of species **8** should be formed.

As illustrated in Figure 5, structure **12** can evolve to yield species **5**, that would eventually dissociate into  $NH + HCO^+$ . These should be the dominant products of the reaction, because, although species **12** can also isomerize to yield species **1** through the intermediate **11** (see Figure 2b), the activation barriers along this pathway are substantially larger than those involved in the **12**–**5** isomerization process. Unfortunately, and to the best of our knowledge, there are no experimental results for this reaction to compare with.

Figure 2a also shows that the barriers for the isomerization of the alternative local minima **8** lie above the entrance channel, so one must conclude that this species, play no role in the reactions between  $OH^+ + HCN$  since it should preferentially dissociate into the reactants.

The situation is slightly different in the case of the  $OH^+ + CNH$  reactions. The most stable structure formed by the interaction of these reactants is species **13**, while structure **7**, which corresponds to the nitrogen attachment lies almost 70 kcal/mol higher in energy. Once species **13** is formed it can evolve either to yield the global minimum of the PES **14**, which would eventually dissociate into  $NH_2^+ + CO$  or to yield species **5**, that would dissociate into  $NH + HCO^+$ . Hence, we must

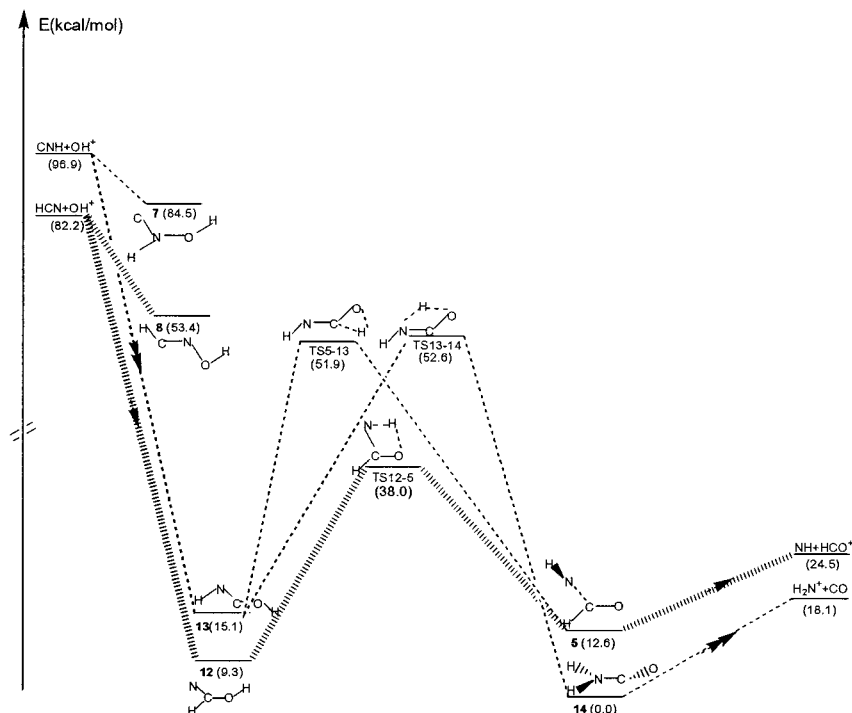


**Figure 5.** Energy profile corresponding to the reactions between  $\text{OH}^+$  with HCN and CNH.

conclude that in  $\text{OH}^+ + \text{CNH}$  reactions, the main ionic products should be  $\text{HCO}^+$  and  $\text{NH}_2^+$ . Again, in this case there is no experimental information to compare with.

**$\text{NO}^+ + \text{CH}_2(^3\text{B}_1)$  and  $\text{CH}_2(^2\text{A}_1) + \text{NO}$  Reactions.** As shown in Figure 2a in both  $\text{NO}^+ + \text{CH}_2$  and  $\text{CH}_2^+ + \text{NO}$  reactions the attachment of the  $\text{CH}_2$  moiety to the nitrogen atom of the NO to yield species **6** is 20 kcal/mol more favorable than the attachment to the oxygen atom, to yield structure **1**. We have already discussed, when dealing with the  $\text{N}^+ + \text{H}_2\text{CO}$  reactions, the reactive processes associated with this latter structure. Therefore, we concentrate now our attention on the most stable isomer **6**. A 1,2-H and a 1,3-H shifts connect this structure with the local minima **4** and **8**, respectively. However, the corresponding activation barriers lie higher in energy than the  $\text{NO}^+ + \text{CH}_2$  dissociation limit. On the other hand, we have found that this dissociation process takes place without activation barrier, i.e., the most favorable process once structure **6** is formed is its dissociation into  $\text{CH}_2 + \text{NO}^+$ . This means that, in  $\text{CH}_2^+ + \text{NO}$  reactions, only the charge exchange channel should be open, in agreement with the experimental observations,<sup>15</sup> while no reaction should be observed in  $\text{NO}^+ + \text{CH}_2$  interactions. Unfortunately, there is no experimental information for this latter process. It must also be noted that we have only explored the triplet potential energy surface, and that the interaction between  $\text{CH}_2^+$  and NO, which are doublet state systems, would take place preferentially with an overall singlet multiplicity.

## Conclusions

We have carried out a systematic survey of the  $[\text{H}_2, \text{C}, \text{N}, \text{O}]^+$  PES in its triplet state multiplicity in order to gain some understanding on the mechanisms associated with several reactions of interest in atmospheric and interstellar chemistry.

We conclude that in  $\text{N}^+(^3\text{P}) + \text{H}_2\text{CO}$  reactions, only a reduced number of structures play a significant role. The predominant products are a consequence of a competitive dissociation of the  $\text{H}_2\text{CON}^+$  cation (**1**) into  $\text{NO}^+ + \text{H}_2\text{C}$  and  $\text{N} + \text{H}_2\text{CO}^+$ . Although the first process is more exothermic than the second

one, the  $\text{N} + \text{H}_2\text{CO}^+$  could be the dominant products, because the dissociation into  $\text{NO}^+ + \text{H}_2\text{C}$  involves a conical intersection and implies a certain activation barrier. Nevertheless, our estimates do not sustain the large difference estimated from the mass spectrometry study. These estimates are affected, however, by a large error and very likely the difference between the proportions in which  $\text{NO}^+$  and  $\text{H}_2\text{CO}^+$  are formed is much smaller. Other products of the reaction are  $\text{NH} + \text{HCO}^+$ , which can be the result of the dissociation of the  $\text{HCONH}^+$  cation (**2**) or the result of the direct dissociation of complex **5**. The first of these processes involves also a conical intersection. According to our estimates, the formation of other possible products as  $\text{CNH} + \text{OH}^+$ ,  $\text{HCN} + \text{OH}^+$ , and  $\text{CO} + \text{NH}_2^+$ , although exothermic, should not be observed since the corresponding reaction pathways involve much higher activation barriers than the previous ones. These conclusions are in good agreement with the experimental evidence.<sup>6</sup>

The characteristics of the  $[\text{H}_2, \text{C}, \text{N}, \text{O}]^+$  PES also explain why no reaction is observed when  $\text{NH}_2^+$  and CO or  $\text{CH}_2$  and  $\text{NO}^+$  interact in the gas phase, while in  $\text{CH}_2^+ + \text{NO}$  reactions, only the charge exchange channel is open.

We can also predict that the dominant products in  $\text{OH}^+ + \text{HCN}$  reactions should be  $\text{NH} + \text{HCO}^+$ . However, when the interaction takes place between  $\text{OH}^+$  and CNH the observed products should be, not only  $\text{NH} + \text{HCO}^+$ , but also  $\text{NH}_2^+ + \text{CO}$ . Unfortunately these reactions have not been experimentally studied.

Finally, it is also worth mentioning that both HCN and CNH behave as carbon bases when the reference acid is  $\text{OH}^+$ .

**Acknowledgment.** This work has been partially supported by the DGES Project PB96-0067 and by the Acci3n Integrada Hispano-Marroqu3 between the Departamento de Qu3mica de la Universidad Aut3noma de Madrid and the Universit3 de Marrakech.

## References and Notes

- (1) For instance, see: (a) Hop, C. E. A.; Chen, H.; Ruttink, P. J. A.; Holmes, J. L. *Org. Mass. Spectrom.* **1991**, *26*, 679. (b) Bohme, D. K. *Chem.*

Rev. **1992**, 92, 1487. (c) Lias, S. G.; Bartmess, J. E.; Liebman, J. F.; Holmes, J. L.; Levin, R. D.; Mallard, W. G. *J. Phys. Chem. Ref. Data* **1988**, 17, Suppl. 1.

(2) See for instance, (a) Chen, W.; Novick, S. E.; McCarthy, M. C.; Thaddeus, P. *J. Chem. Phys.* **1998**, 109, 10190. (b) Apponi, A. J.; McCarthy, M. C.; Gottlieb, C. A.; Thaddeus, P. *J. Chem. Phys.* **1999**, 111, 3911. (c) Apponi, A. J.; McCarthy, M. C.; Gottlieb, C. A.; Thaddeus, P. *Astrophys. J. Lett.* **1999**, 516, L103. (d) Bell, M.; Feldmann, P. A.; Travers, M. J.; McCarthy, M. C.; Gottlieb, C. A.; Thaddeus, P. *Astrophys. J.* **1997**, 483, L61. (e) McCarthy, M. C.; Travers, M. J.; Kovacs, A.; Chen, W.; Novick, S. E.; Gottlieb, C. A.; Thaddeus, P. *Science* **1997**, 275, 518.

(3) (a) Curtiss, L. A.; Raghavachari, K.; Trucks, G. W.; Pople, J. A. *J. Chem. Phys.* **1991**, 94, 7221. (b) Ochterski, J. W.; Petersson, G. A.; Montgomery, J. A., Jr. *J. Chem. Phys.* **1996**, 104, 2598.

(4) (a) Esseffar, M.; Luna, A.; M6, O.; Y6ñez, M. *J. Phys. Chem.* **1993**, 97, 6607. (b) Luna, A.; Y6ñez, M. *J. Phys. Chem.* **1993**, 97, 10659. (c) Luna, A.; Manuel, M.; M6, O.; Y6ñez, M. *J. Phys. Chem.* **1994**, 98, 6980. (d) Esseffar, M.; Luna, A.; M6, O.; Y6ñez, M. *J. Phys. Chem.* **1994**, 98, 8679. (e) Manuel, M.; M6, O.; Y6ñez, M. *J. Phys. Chem.* **1997**, 101, 1722. (f) Manuel, M.; M6, O.; Y6ñez, M. *Mol. Phys.* **1997**, 91, 503. (g) Manuel, M.; M6, O.; Y6ñez, M. *Mol. Phys.* **1999**, 96, 231. (h) Gonz6lez, A. I.; M6, O.; Y6ñez, M. *Int. J. Mass Spectrom.* **1998**, 179/180, 77. (i) Gonz6lez, A. I.; Luna, A.; Y6ñez, M. *J. Phys. Chem. A* **1999**, 103, 4543.

(5) (a) Ferguson, E. E. *Atmospheres of Earth and the Planets*; McCormac, B. M., Ed.; Reidel: Dordrecht, 1975. (b) Thomas, L. *Radio Sci.* **1974**, 9, 121.

(6) (a) Smith, D.; Adams, N. G.; Miller, T. M. *J. Chem. Phys.* **1978**, 69, 308. (b) Adams, N. G.; Smith, D.; Paulson, J. F. *J. Chem. Phys.* **1980**, 72, 288.

(7) Frisch, M. J.; Trucks, G. W.; Schlegel, H. B.; Scuseria, G. E.; Robb, M. A.; Cheeseman, J. R.; Zakrzewski, V. G.; Montgomery, J. A., Jr.; Stratmann, R. E.; Burant, J. C.; Dapprich, S.; Millam, J. M.; Daniels, A. D.; Kudin, K. N.; Strain, M. C.; Farkas, O.; Tomasi, J.; Barone, V.; Cossi, M.; Cammi, R.; Mennucci, B.; Pomelli, C.; Adamo, C.; Clifford, S.; Ochterski, J.; Peterson, G. A.; Ayala, P. Y.; Cui, Q.; Morokuma, K.; Malick, D. K.; Rabuck, A. D.; Raghavachari, K.; Foresman, J. B.; Cioslowski, J.; Ortiz, J. V.; Baboul, A. G.; Stefanov, B. B.; Liu, G.; Liashenko, A.; Piskorz, P.; Komaromi, I.; Gomperts, R.; Martin, R. L.; Fox, D. J.; Keith, T. A.; Al-Laham, M. A.; Peng, C. Y.; Nanayaklara, A.; Gonzalez, C.; Challacombe, M.; Gill, P. M. W.; Johnson, B. J.; Chen, W.; Wong, M. W.; Andres, J. L.; Head-Gordon, M.; Replogle, E. S.; Pople, J. A. *Gaussian 98*, Revision A.7; Gaussian, Inc.: Pittsburgh, PA, 1998.

(8) Bearpark, M. J.; Robb, M. A.; Schlegel, H. B. *Chem. Phys. Lett.* **1994**, 223, 269.

(9) Weinhold, F.; Carpenter, J. E. *The Structure of Small Molecules and Ions*; Plenum: New York, 1988.

(10) (a) Bader, R. F. W.; Ess6n, H. *J. Chem. Phys.* **1984**, 80, 1943. (b) Bader, R. F. W.; MacDougall, P. J.; Lau, C. D. *J. Am. Chem. Soc.* **1984**, 106, 1594. (c) Bader, R. F. W. *Atoms in Molecules. A Quantum Theory*; Oxford University Press: New York, 1990.

(11) Cremer, D.; Kraka, E. *Angew. Chem.* **1984**, 96, 612.

(12) The AIM-PAC program package has been provided by J. Cheeseman and R. F. W. Bader.

(13) Esseffar, M.; Luna, A.; M6, O.; Y6ñez, M. *Chem. Phys. Lett.* **1994**, 223, 240.

(14) Anicich, V. G. *J. Phys. Chem. Ref. Data* **1993**, 22, 1469.

(15) Viggiano, A. A.; Howark, F.; Albritton, D. L.; Fehsenfeld, F. C.; Adams, N. G.; Smith, D. *Astrophys. J.* **1980**, 236, 492.